

L-Dopa Modulates Functional Connectivity in Striatal Cognitive and Motor Networks: A Double-Blind Placebo-Controlled Study

Clare Kelly,¹ Greig de Zubicaray,³ Adriana Di Martino,^{1,5} David A. Copland,⁴ Philip T. Reiss,^{2,6} Donald F. Klein,^{1,6,7} F. Xavier Castellanos,^{1,6} Michael P. Milham,¹ and Katie McMahon³

¹Phyllis Green and Randolph Cowen Institute for Pediatric Neuroscience, and ²Division of Biostatistics, New York University Child Study Center, New York, New York 10016, ³Centre for Magnetic Resonance and ⁴Centre for Clinical Research and School of Health and Rehabilitation Sciences, University of Queensland, Brisbane, Queensland 4072, Australia, ⁵Division of Child and Adolescent Neuropsychiatry, Department of Neuroscience, University of Cagliari, 09126 Cagliari, Italy, ⁶Nathan S. Kline Institute for Psychiatric Research, Orangeburg, New York 10962, and ⁷Department of Psychiatry, College of Physicians and Surgeons, Columbia University, New York, New York 10032

Functional connectivity (FC) analyses of resting-state fMRI data allow for the mapping of large-scale functional networks, and provide a novel means of examining the impact of dopaminergic challenge. Here, using a double-blind, placebo-controlled design, we examined the effect of L-dopa, a dopamine precursor, on striatal resting-state FC in 19 healthy young adults. We examined the FC of 6 striatal regions of interest (ROIs) previously shown to elicit networks known to be associated with motivational, cognitive and motor subdivisions of the caudate and putamen (Di Martino et al., 2008). In addition to replicating the previously demonstrated patterns of striatal FC, we observed robust effects of L-dopa. Specifically, L-dopa increased FC in motor pathways connecting the putamen ROIs with the cerebellum and brainstem. Although L-dopa also increased FC between the inferior ventral striatum and ventrolateral prefrontal cortex, it disrupted ventral striatal and dorsal caudate FC with the default mode network. These alterations in FC are consistent with studies that have demonstrated dopaminergic modulation of cognitive and motor striatal networks in healthy participants. Recent studies have demonstrated altered resting state FC in several conditions believed to be characterized by abnormal dopaminergic neurotransmission. Our findings suggest that the application of similar experimental pharmacological manipulations in such populations may further our understanding of the role of dopaminergic neurotransmission in those conditions.

Introduction

Functional connectivity (FC) analyses of resting-state fMRI data (Biswal et al., 1995) have recently provided novel insights into the brain's functional architecture. Region of interest (ROI)-based analyses elicit detailed maps of FC, which recapitulate functional distinctions within regions such as the anterior cingulate (Margulies et al., 2007), striatum (Di Martino et al., 2008) and hippocampus (Kahn et al., 2008). Furthermore, disrupted FC has been observed in several clinical conditions, including ADHD, schizophrenia and Alzheimer's disease, as well as in normal aging (Greicius et al., 2004; Andrews-Hanna et al., 2007; Zhou et al., 2007; Castellanos et al., 2008). Resting state FC approaches thus provide an ideal complement to, but not a replacement for, task-

based approaches for mapping brain circuits in healthy and pathological populations.

Dopaminergic modulation of neuronal communication is crucial to normal functioning of brain circuits subserving thought and behavior (Montague et al., 2004; Robbins, 2005). Abnormal dopaminergic neurotransmission, particularly in striatal circuits, is associated with the alterations in thought, mood and behavior observed in many pathological conditions, as well as in normal aging (Bäckman et al., 2006; Graybiel, 2008). Resting state FC approaches offer an ideal means for interrogating large-scale striatal networks. Furthermore, the disruption of FC in populations characterized by dopamine (DA) abnormalities prompts the hypothesis that DA may play a role in the regulation of FC in striatal circuits.

We evaluated this hypothesis, through an examination of the effects of DA challenge on striatal FC. Previous studies suggest that DA manipulations can modulate both task-based (Honey et al., 2003; Nagano-Saito et al., 2008) and resting state FC (Li et al., 2000; Achard and Bullmore, 2007). Recently, we mapped the FC of six ROIs placed throughout caudate and putamen (Di Martino et al., 2008). We observed distinct patterns of FC for each seed, which paralleled motivational, cognitive and motor subdivisions predicted by models of striatal circuitry (Alexander et al., 1986;

Received Feb. 17, 2009; revised March 30, 2009; accepted April 2, 2009.

This work was supported by an Australian Research Council (ARC) Discovery grant (DP0452264) awarded to D.A.C. and K.M., and by a National Institute on Drug Abuse grant (1R03DA024775-01) awarded to C.K.

The authors declare no competing interests.

Correspondence should be addressed to either of the following: Dr. Katie McMahon, Centre for Magnetic Resonance, University of Queensland, Brisbane, QLD 4072, Australia. E-mail: katie.mcmahon@cmr.uq.edu.au; or Dr. Michael P. Milham, New York University Child Study Center, 215 Lexington Avenue, 14th Floor, New York, NY 10016, E-mail: michael.milham@nyumc.org.

DOI:10.1523/JNEUROSCI.0810-09.2009

Copyright © 2009 Society for Neuroscience 0270-6474/09/297364-15\$15.00/0

Haber, 2003), and which were consistent with a meta-analysis of corticostriatal coactivation across 126 task-based neuroimaging studies (Postuma and Dagher, 2006). Here, we applied the same systematic seeding approach to examine the effects of the DA metabolic precursor, L-dihydroxyphenylalanine (L-dopa) on resting state FC in 19 young adults, using a double-blind, placebo-controlled design. To our knowledge, this is the first study to use such a design to investigate the effects of a DA manipulation on seed-based resting-state FC.

We predicted that the previously observed patterns of striatal FC observed would be replicated in the placebo condition, but altered by L-dopa. Studies in PD patients suggest L-dopa improves or normalizes function within motor networks (Haslinger et al., 2001; Buhmann et al., 2003). We hypothesized that L-dopa would increase FC between striatal motor regions (putamen) and subcortical and cortical regions associated with motor function. Given studies demonstrating that L-dopa modulates task-evoked activation within frontostriatal circuits (Mattay et al., 2002; Rowe et al., 2008), and can improve performance on tasks that rely on those circuits (Cools, 2006), we hypothesized that L-dopa would also alter FC between caudate and prefrontal cortex.

Materials and Methods

Participants

Twenty healthy adults (8 females; mean age = 27.3 years), free from a history of neurological or psychiatric illness and psychotropic medications, contraindications to MRI or Madopar (L-dopa), participated in this study. Volunteers completed a medical questionnaire and interview with a recruiting nurse. One participant showed abnormally high L-dopa serum levels in the placebo condition (16,400 pmol/L), and was excluded from the study (19 remaining participants; mean age = 26.2 years, 7 females). Participants were reimbursed Au\$30 to cover their travel costs. All procedures were reviewed and approved by the institutional review board of Queensland University.

Design

Participants were assigned to receive either placebo or L-dopa in session 1 and the other treatment in session 2 at least 2 weeks later, in a randomized double-blind, placebo controlled crossover design. L-dopa was administered in the form of a Madopar capsule containing 100 mg of levodopa (L-dopa) and 25 mg of benserazide (a peripheral decarboxylase blocker) by a research nurse. The dose was identical to that used previously in psychopharmacological studies reporting behavioral effects (e.g., Kisichka et al., 1996; Angwin et al., 2004; Copland et al., 2009). Participants were scanned early in the morning and were advised not to eat breakfast since food may affect absorption rates. Placebo was administered in identical capsules. Functional imaging took place ~45 min after ingestion of the capsule, consistent with peak plasma L-dopa levels (Olanow et al., 2000). Blood pressure and heart rate were measured before capsule ingestion and after the imaging session. Blood was taken immediately before the imaging session and plasma DA levels measured via gas chromatography/mass spectrometry. Participants also completed a standardized self-report measure of subjective feelings (e.g., alertness, lethargy, tension) before the imaging session (Bond and Lader, 1974).

Functional imaging

Functional imaging data were acquired using a 4T Bruker MedSpec system equipped with a transverse electromagnetic head coil (Vaughan et al., 2002). We collected one “resting state” scan, comprising 200 contiguous echo planar imaging (EPI) whole-brain functional volumes (TR = 2100 ms; TE = 30 ms; flip angle = 90°, 36 slices, matrix = 64 × 64; acquisition voxel size = 3.6 × 3.6 × 3.6 mm). During this scan participants were asked to relax with their eyes open. Before the resting-state scan, a point-spread function (PSF) mapping sequence was acquired to correct geometric distortions in the EPI volumes (Zaitsev et al., 2003). A high-resolution T1-weighted anatomical image was also acquired using a magnetization prepared gradient echo sequence (TR = 2500 ms; TE =

3.83 ms; TI = 1500 ms; flip angle = 8°; 256 slices, acquisition voxel size = 0.9 × 0.9 × 0.9 mm).

Image preprocessing and individual analyses

AFNI (Cox, 1996) was used to perform the initial preprocessing steps of slice timing, correction for interleaved acquisition (using Fourier-space time-series phase-shifting) and motion correction (by aligning each volume to a “base” image using Fourier interpolation). The first five volumes were discarded to allow for magnetization equilibration. All other data processing was performed using FSL (www.fmrib.ox.ac.uk). Further image preprocessing comprised spatial smoothing (using a Gaussian kernel of FWHM 5 mm), mean-based intensity normalization of all volumes by the same factor [each subject’s entire four-dimensional (4-D) dataset was scaled by its global mean], and temporal bandpass filtering (high-pass temporal filtering: Gaussian-weighted least-squares straight line fitting, with $\sigma = 100.0$ s; Gaussian low-pass temporal filtering HWHM 2.8 s). Registration of high-resolution structural images to the MNI152 template (Montreal Neurological Institute) with 1 mm³ resolution was performed using the FSL linear registration tool FLIRT (Jenkinson and Smith, 2001; Jenkinson et al., 2002). Transformation to MNI152 standard space was then further refined using FNIRT nonlinear registration (Andersson et al., 2007a,b). Linear registration of each participant’s functional timeseries to the space of the high-resolution structural image, was also performed using FLIRT.

Movement parameters

Movement in each of the cardinal directions (X, Y and Z), and rotational movement around 3 axes (pitch, yaw and roll) were calculated for each participant. Data were also visually inspected for movement-related artifacts.

Functional connectivity

Nuisance signal regression. To control for the effects of physiological processes (such as fluctuations related to cardiac and respiratory cycles), and motion, we removed signal associated with several nuisance covariates. Specifically, we regressed each subject’s 4-D volume on nine predictors that modeled nuisance signals from white matter (WM), CSF, the global signal, and six motion parameters. Correction for time series autocorrelation (prewhitening) was performed. The six motion covariates were generated as part of the output of the AFNI motion correction program 3dvolreg. The global signal regressor was generated by averaging across all voxels within the brain. Finally, to generate the WM and CSF nuisance covariates, we first segmented each individual’s high-resolution structural image, using the FAST segmentation program provided by FSL. The resulting segmented WM and CSF images were then thresholded to ensure 80% tissue type probability. These thresholded masks were then applied to each individual’s time series, and a mean time series was calculated by averaging across all voxels within the mask.

This nuisance signal regression step produced prewhitened, 4-D residuals for each participant. Voxelwise scaling was performed on the 4-D residuals, by dividing each voxel’s time series by its SD. Performing this step ensures that the ensuing FC estimates represent partial correlations rather than regression parameter estimates (e.g., Vincent et al., 2006), and removes potential between-condition differences in the magnitude of BOLD fluctuations (Sorg et al., 2007). As a final preprocessing step, each participant’s time series was spatially normalized by applying the previously computed transformation to MNI152 standard space, with 1 mm³ resolution. Specifically, the linear function describing the transformation from functional to high-resolution structural space was applied to each participant’s scaled residuals volume using FLIRT. Subsequent to this initial linear coregistration step, the nonlinear warping transformations derived for that participant’s high-resolution structural image were applied to the functional volume, to produce a scaled residuals volume in MNI152 space, with 1 × 1 × 1 mm resolution.

ROI selection and seed generation. We used the same 12 striatal seeds (six in each hemisphere) described by Di Martino et al. (2008). Each seed ROI was approximately spherical (volume = 257 × 1 mm³ voxels, radius ~4 mm). These were located (in MNI152 space) in the (1) inferior ventral striatum (VSi) ($\pm 9 -8$, corresponding to the nucleus accumbens), (2) superior ventral striatum (VSs) ($\pm 10 15 0$, corresponding to the

ventral caudate), (3) dorsal caudate (DC) ($\pm 13\ 15\ 9$), (4) dorsal caudal putamen (dcP) ($\pm 28\ 1\ 3$), (5) dorsal rostral putamen (drP), ($\pm 25\ 8\ 6$), and (6) the ventral rostral putamen (vrP) ($\pm 20\ 12\ -3$). As outlined in detail by Di Martino et al. (2008), these seed locations are consistent with both anatomical and functional subdivisions of the striatum (Heimer and Alheid, 1991; Drevets et al., 1999; Postuma and Dagher, 2006). The 12 seed ROIs were applied to each participant's prewhitened, 4-D residuals, and a mean time series was calculated for each seed by averaging across all voxels within the seed.

To further confirm the anatomical validity of our findings, and to control for potential interindividual anatomic variability, we conducted additional probability-weighted seed-based analyses of the striatum. We created right- and left-hemisphere masks for the nucleus accumbens, caudate, and putamen, as defined by the Harvard–Oxford Structural Atlas, a validated probabilistic atlas included with FSL, which parcellates each hemisphere into anatomically distinct cortical and subcortical regions (Kennedy et al., 1998; Makris et al., 1999). In this atlas, every voxel is assigned a value that corresponds to its probability of belonging to a given anatomical region (e.g., caudate). To control for potential interindividual anatomic variability for each striatal region, we used these probability values to weight each voxel's time series within that region (Stark et al., 2008). Mean time series were then extracted for each striatal region by averaging across all probability-weighted time series within that region, for each participant.

Seed-based functional connectivity analyses

We performed 12 separate multiple regression analyses in which we regressed each subject's 4-D residuals volume on each of the 12 seed time series, using the FSL program FEAT. These analyses produced subject-level maps of all voxels that were positively and negatively correlated with the seed time series. The same procedure was followed for the six probability-weighted ROIs.

Group-level analyses

Analyses of group-level FC for the L-dopa and placebo conditions, and pairwise L-dopa vs placebo comparisons were performed using a repeated-measures mixed-effects ordinary least-squares model as implemented in FSL. This group-level analysis produced thresholded Z-score maps ("networks") of positive and negative connectivity for each striatal ROI and for each condition. Direct voxelwise condition comparisons produced thresholded Z-score maps of those voxels that showed significant L-dopa-related changes in FC with each ROI. For all analyses, corrections for multiple comparisons were performed at the cluster level using Gaussian random field theory (min $Z > 2.3$; cluster significance: $p < 0.05$, corrected).

Results

Blood plasma DA levels were higher on L-dopa (mean 7145 pmol/L) compared with placebo (mean 302 pmol/L). Self-rated subjective mood did not differ significantly on L-dopa versus placebo, nor did blood pressure or heart rate ($p > 0.05$).

Movement

The root mean square (rms) of the movement parameters did not exceed 1 mm or 1° in any of the cardinal directions or rotational axes. There were no significant differences between conditions in the mean, maximum or rms of the movement parameters.

Striatal functional connectivity: placebo

Relative to our previous study of striatal FC (Di Martino et al., 2008), the present data were acquired from a different set of participants, in a different magnet of different field strength. Nonetheless, the patterns of functional connectivity observed for the placebo condition were remarkably consistent with those previously observed by Di Martino et al. (Figs. 1–4; supplemental Table S1, available at www.jneurosci.org as supplemental material). The three putamen seeds exhibited positive correlations

with secondary motor cortical and subcortical regions, as well as prefrontal associative regions. Within the putamen, the network associated with the ventral seed (vrP) comprised more extensive regions of PFC than did the dorsal seeds (dcP and drP), which demonstrated correlations with superior premotor areas, the supramarginal and angular gyri that were not observed for the vrP seed (Figs. 1, 2).

In the caudate, we replicated the ventral-dorsal distinction previously observed by Di Martino et al. (2008). Whereas the more dorsal caudate seeds (DC and VSs) were associated with more dorsal areas of lateral and medial PFC, the VSi seed was primarily correlated with limbic regions (Figs. 3, 4). In supplemental Results A (available at www.jneurosci.org as supplemental material), we address in greater detail differences between the present set of analyses and those of Di Martino et al. (2008). Furthermore, because we did not have specific predictions concerning the effect of L-dopa on the negative FC of the striatum, we do not explicitly discuss the patterns of negative functional connectivity in the main text. However, the patterns of negative FC observed were consistent with those previously observed by Di Martino et al. (2008), and are shown in supplemental Figures S1–S4 (see also supplemental Results A and Fig. S5, available at www.jneurosci.org as supplemental material). Note that no significant effects of L-dopa on negative functional connectivity were observed, for any of the ROIs examined.

L-Dopa versus placebo: putamen

We performed direct comparisons of FC in the L-dopa and placebo conditions using a repeated-measures mixed-effects model. These analyses produced thresholded Z-score maps of those voxels that showed significant L-dopa-related changes in FC with each ROI (min $Z > 2.3$; cluster significance: $p < 0.05$, corrected). Although the broad patterns of connectivity were highly similar for both the placebo and L-dopa conditions, we observed significantly stronger connectivity between all six putamen seeds and the anterior cerebellum and cerebellar vermis, in the L-dopa condition (Figs. 1–4; supplemental Fig. S6, available at www.jneurosci.org as supplemental material; Table 1) (cerebellar nomenclature derived from Schmahmann et al., 2000). Additionally, the right hemisphere ventral putamen seed, vrP exhibited increased connectivity with the dorsal midbrain and ventral brainstem (proximal to the pons), and all three left hemisphere putamen seeds exhibited increased connectivity with this ventral brainstem region. No regions of L-dopa-related decreases in functional connectivity were observed, nor were any significant differences in negative connectivity for any of the putamen seeds observed.

L-Dopa versus placebo: caudate

The group-level map of DC connectivity in the L-dopa condition (Figs. 3, 4) showed a striking reduction in connectivity between right DC and regions of the default mode network (see also supplemental Fig. S7, available at www.jneurosci.org as supplemental material). This was supported by direct comparisons, which revealed stronger correlations between the right DC and the posterior cingulate, ventromedial and dorsomedial PFC for placebo, relative to L-dopa. Significantly greater connectivity was also observed between both right and left VSs and posterior cingulate cortex (PCC), and between right and left VSi and PCC and medial occipital cortex (Figs. 3, 4; Table 2), for placebo, relative to L-dopa.

In the group-level maps of FC for the caudate ROIs, increased connectivity with lateral PFC in the L-dopa condition, relative to placebo is apparent (Figs. 3, 4, which show the group-level con-

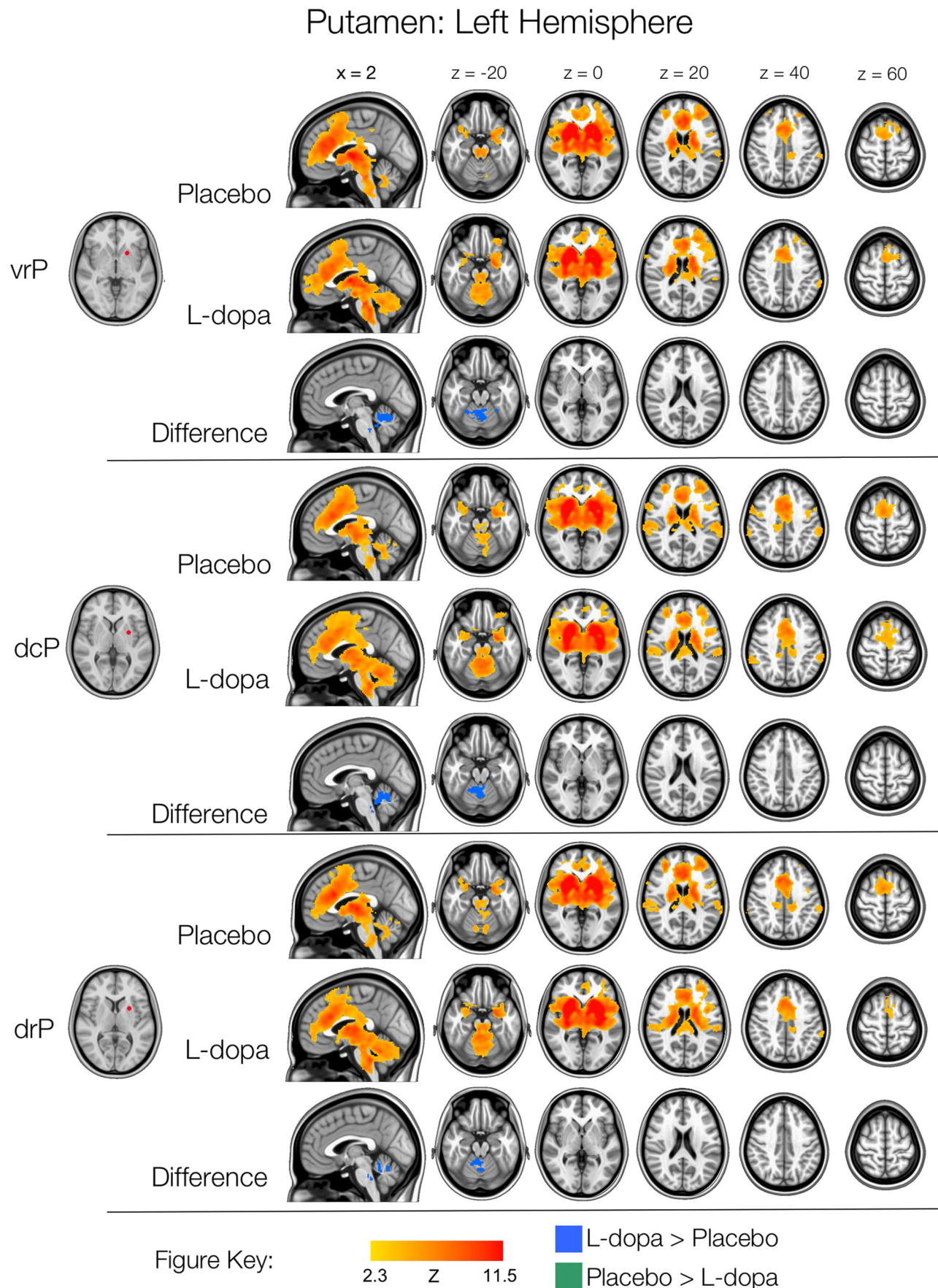


Figure 1. Left hemisphere putamen functional connectivity. Thresholded Z-score maps ($\min Z > 2.3$; cluster significance: $p < 0.05$, corrected) of positive functional connectivity for each condition, and significant L-dopa-related increases and decreases in functional connectivity. Images are displayed according to radiological convention (left is right).

Putamen: Right Hemisphere

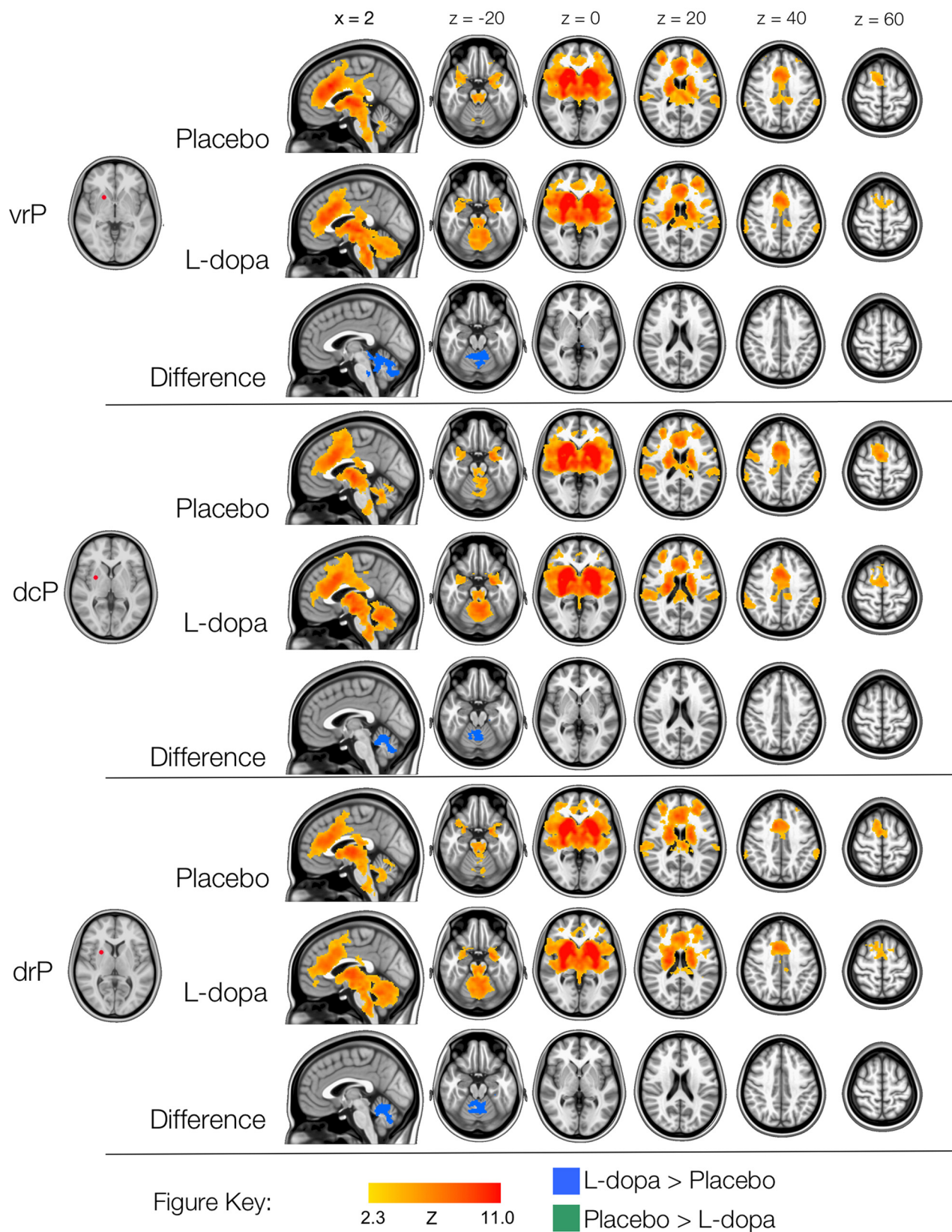


Figure 2. Right hemisphere putamen functional connectivity. Thresholded Z-score maps ($\min Z > 2.3$; cluster significance: $p < 0.05$, corrected) of positive functional connectivity for each condition, and significant L-dopa-related increases and decreases in functional connectivity. Images are displayed according to radiological convention (left is right).

Caudate: Left Hemisphere

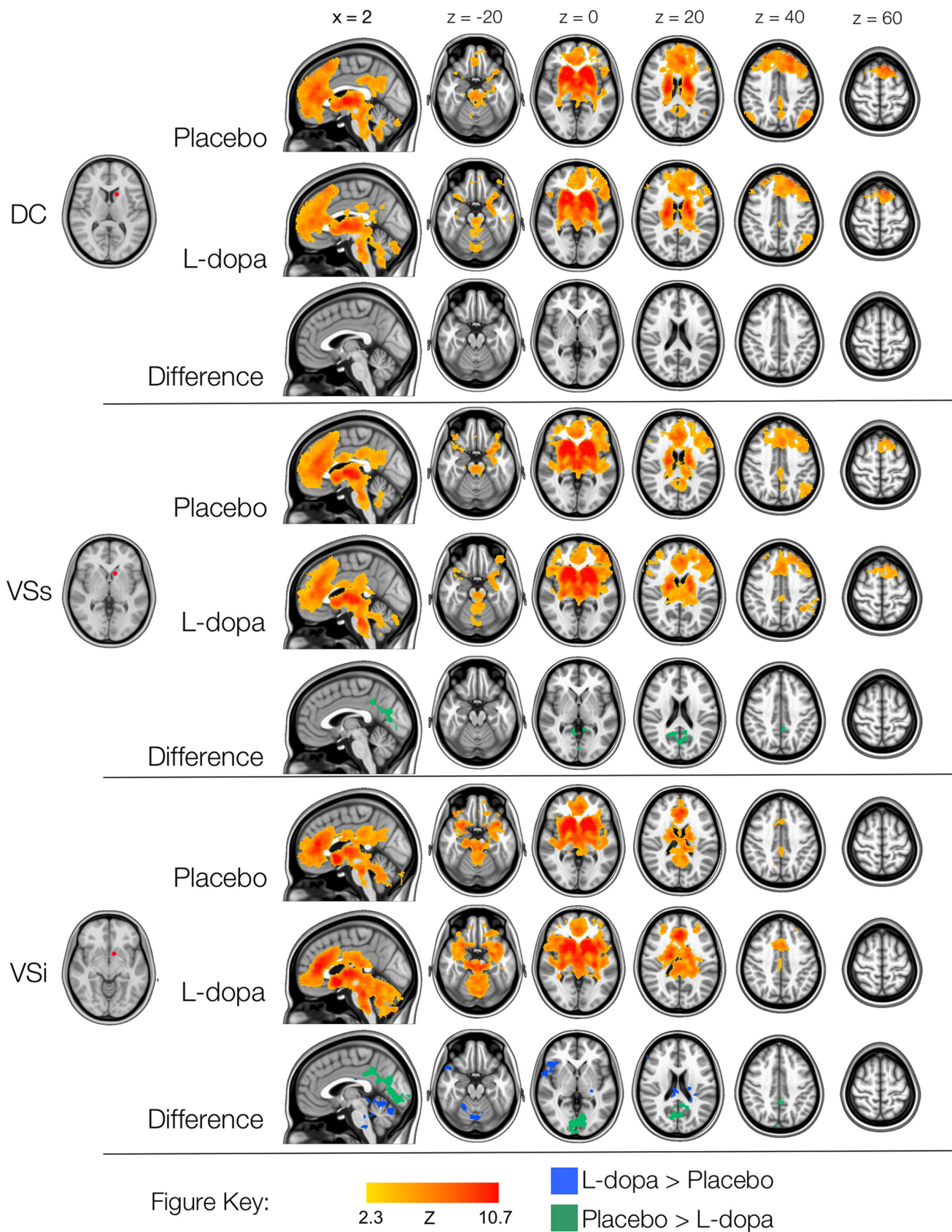


Figure 3. Left hemisphere caudate functional connectivity. Thresholded Z-score maps of positive functional connectivity for each condition, and significant L-dopa-related increases and decreases in functional connectivity. Images are displayed according to radiological convention (left is right).

Caudate: Right Hemisphere

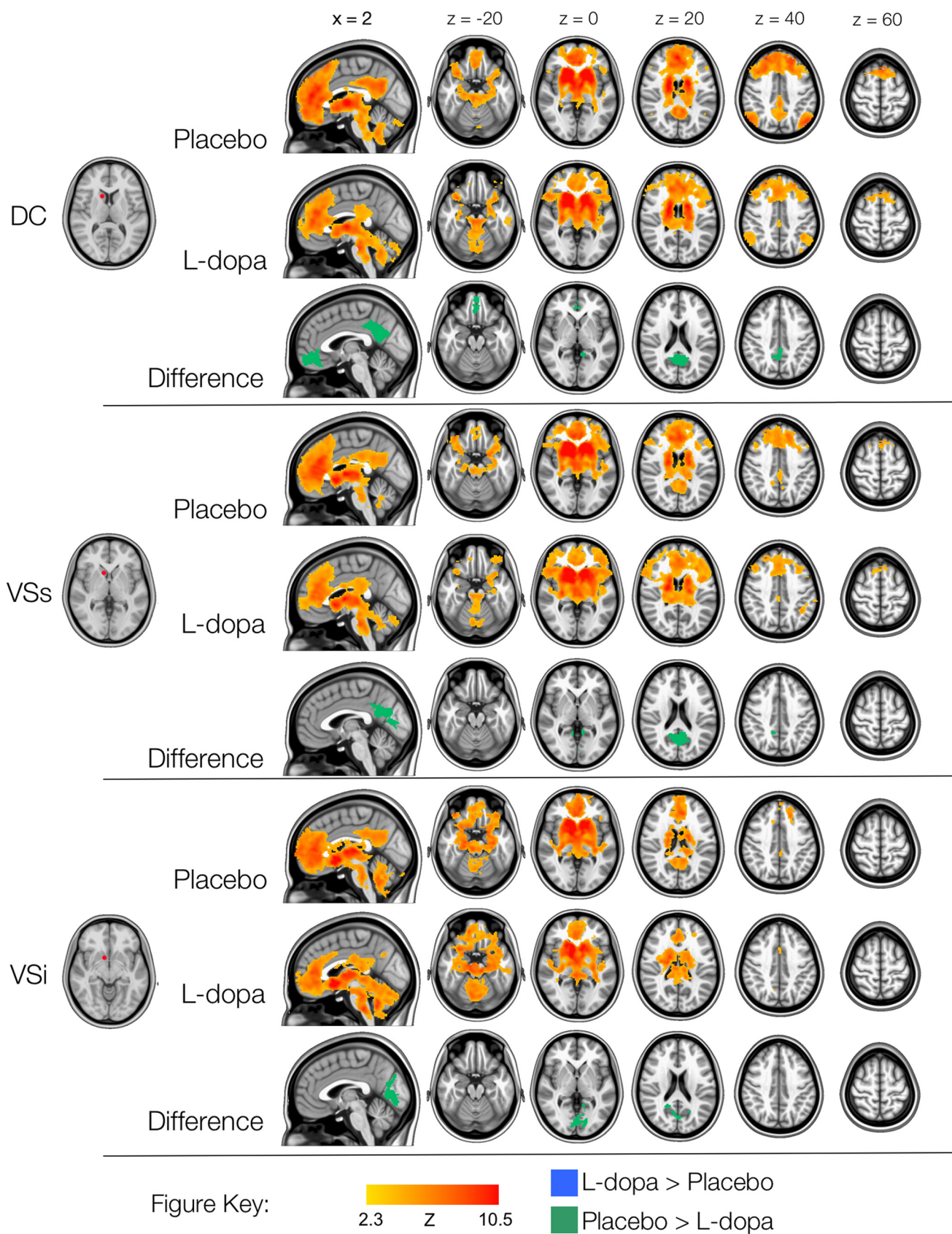


Figure 4. Right hemisphere caudate functional connectivity. Thresholded Z-score maps of positive functional connectivity for each condition, and significant L-dopa-related increases and decreases in functional connectivity. Images are displayed according to radiological convention (left is right).

Table 1. Significant increases in putamen functional connectivity for L-dopa, relative to placebo (min Z > 2.3; cluster significance: p < 0.05, corrected), as shown in Figures 1 and 2

| Region | | mm ³ | Peak voxel | | |
|--------|--|-----------------|------------|-----|-----|
| | | | x | y | z |
| L dcP | L cerebellum (lobules III, IV, V), cerebellar vermis (lobules V, VI, VIII, VIIIa, VIIIb), brainstem (pons) | 1611 | -12 | -40 | -32 |
| R dcP | L cerebellum (lobules IV, V) | 1122 | -2 | -70 | -36 |
| L drP | L cerebellum (lobules III, IV, V), vermis (lobule VI) | 924 | -12 | -40 | -34 |
| R drP | BL cerebellum (lobules III, IV, V, X), vermis (lobules VI, VIIIa), brainstem (pons) | 1689 | 8 | -62 | -18 |
| L vrP | L cerebellum (lobules III, IV, V), vermis (lobule VI), brainstem (pons) | 1150 | -12 | -38 | -34 |
| R vrP | L cerebellum (lobules III, IV, V, IX, VIIIb), vermis (VI, VIIb, VIIIa), dorsal midbrain, brainstem (pons) | 2322 | -24 | -40 | -34 |

Cerebellar nomenclature was derived from Schmahmann et al. (2000). BA, Brodmann area; L, left; R, right.

Table 2. Significant changes in caudate functional connectivity for L-dopa, relative to placebo (min Z > 2.3; cluster significance: p < 0.05, corrected), as shown in Figures 3 and 4

| | | mm ³ | BA | Peak voxel | | |
|--|--|-----------------|----------------------------|------------|-----|-----|
| | | | | x | y | z |
| L-Dopa-related increases in functional connectivity | | | | | | |
| L VSi | BL cerebellum (lobules IV, V, VI), cerebellar vermis (lobule VI), brainstem (pons) | 1135 | | -12 | -32 | -36 |
| R inferior frontal gyrus, anterior insula, superior temporal gyrus | | 709 | 44, 45, 6, 22, 38 | 50 | 26 | 2 |
| L globus pallidus | | 577 | | -30 | -26 | 6 |
| BL cerebellum (lobules V, VI, IX, crus I) | | 512 | | -10 | -66 | -16 |
| L-Dopa-related decreases in functional connectivity | | | | | | |
| R DC | BL PCC | 2029 | 23, 26, 30, 31 | 0 | -40 | 38 |
| | BL ventromedial prefrontal cortex | 984 | 10, 32 | -2 | 40 | -14 |
| L VSs | BL PCC, medial occipital cortex | 1559 | 23, 26, 30, 31, 19 | 18 | -48 | 26 |
| R VSs | BL PCC, medial occipital cortex | 2212 | 23, 26, 30, 31, 19 | -4 | -66 | 24 |
| L VSi | BL PCC, medial occipital cortex | 2546 | 23, 26, 30, 31, 17, 18, 19 | 0 | -80 | -2 |
| R VSi | BL PCC, medial occipital cortex | 1876 | 26, 29, 30, 17, 18, 19 | -14 | -60 | 6 |

BA, Brodmann area; BL, bilateral; L, left; R, right.

nnectivity for the L-dopa and placebo conditions separately, see the top two rows for each seed). In direct comparisons, these differences only reached statistical significance for the left VSi seed: we observed increased FC between left VSi and right inferior prefrontal cortex, as well as between left VSi and the bilateral anterior and right posterior cerebellum, ventral brainstem and globus pallidus (Fig. 3, Table 2).

Because the default mode network is hypothesized to have a negative or even competitive relationship with regions related to attentional control, such as PFC (e.g., Fox et al., 2005; Fransson, 2005; Kelly et al., 2008), we further examined the changes in functional connectivity between left VSi and right vLPFC and between each of the caudate seeds and PCC (a core region of the default mode network) as a result of L-dopa administration. Specifically, we computed the mean difference in FC between the L-dopa and placebo conditions in the right vLPFC region that exhibited significant (i.e., min Z > 2.3; cluster significance: p < 0.05, corrected) L-dopa-related increase in FC with left VSi (Fig. 5). We also computed the mean difference in FC between the L-dopa and placebo conditions in each of the PCC regions (clusters) that exhibited significant L-dopa-related decreases in FC with left VSi, right DC, right VSs and left VSs. We then calculated the correlation, across participants, between the L-dopa-related increase in FC and each of the L-dopa-related decreases. For each pairing, we observed an inverse correlation between the L-dopa-related changes in connectivity (Fig. 5): the greater the L-dopa-related increase in connectivity between left VSi and vLPFC, the greater the L-dopa-related decrease in connectivity for the same participant, between left VSi and PCC ($r = -0.47$, $p < 0.05$), between right DC and PCC ($r = -0.63$, $p < 0.005$), between

right VSs and PCC ($r = -0.47$, $p < 0.05$). The same relationship just escaped significance for left VSs ($r = -0.45$, $p = 0.051$). This inverse relationship was not present for any of the other clusters which demonstrated L-dopa-related increases in connectivity with left VSi (i.e., cerebellum, brainstem and globus pallidus).

Probability-weighted ROIs

Figures 6 and 7 show the patterns of FC observed for the six probability-weighted ROIs, corresponding to the nucleus accumbens, caudate and putamen. The patterns of FC associated with these larger ROIs were highly consistent with those observed for the smaller striatal seeds, albeit with less fine-grained detail, as would be expected for larger ROIs. The effects of L-dopa were also consistent with those observed for the smaller seeds, although more circumscribed (see Table 3). Both right and left nucleus accumbens ROIs exhibited reduced connectivity with posterior cingulate and medial occipital cortices as a result of L-dopa administration. Left nucleus accumbens also exhibited increased FC with (primarily posterior) cerebellum and brainstem, but not with right inferior prefrontal cortex, as was observed for left VSi. The right caudate ROI exhibited reduced FC with PCC, as was observed for the right DC seed. Finally, the putamen ROIs exhibited increased connectivity with regions of left cerebellum, and left putamen also exhibited increased connectivity with the ventral brainstem (left only). No significant differences in negative functional connectivity were observed.

Iterative connectivity analyses

To further explore the striking reductions in connectivity between the caudate and the default mode network in the L-dopa

condition, we performed an additional FC analysis in which we examined the connectivity of the PCC region that demonstrated reduced connectivity with the right hemisphere probability-weighted caudate ROI. We first identified the region within PCC which exhibited the greatest connectivity with the right hemisphere probability-weighted caudate ROI in the placebo, relative to the L-dopa condition (Fig. 7). This peak coordinate ($x = 0, y = -42, z = 38$) then formed the center of a spherical seed ROI (volume = $257 \times 1 \text{ mm}^3$ voxels, radius $\sim 4 \text{ mm}$). Maps of significant positive FC for this PCC seed, and of significant condition-related differences in FC were then generated in the same manner as for each of the primary striatal seed ROIs.

The results of this iterative FC analysis support our primary findings of reduced connectivity between the caudate and regions of the default mode network. We observed a drastic reduction in the connectivity of the default mode network in the L-dopa condition, relative to placebo, particularly for correlations between the caudate and the PCC (Fig. 8). Specifically, L-dopa significantly reduced connectivity between the PCC seed and proximal PCC regions, rostral ACC/medial PFC, ventral striatum and dorsal caudate.

Discussion

The present work is among the first resting state fMRI studies to examine the effects of a placebo-controlled dopaminergic manipulation on FC within large-scale networks (e.g., Achard and Bullmore, 2007). In the placebo condition, we replicated the findings of Di Martino et al. (2008), observing patterns of FC consistent with hypothesized motor (dorsal putamen), cognitive (ventral putamen, dorsal caudate, superior ventral striatum) and affective (inferior ventral striatum) subdivisions of the striatum. In line with our predictions, L-dopa increased FC in motor networks joining putamen and cerebellum and brainstem. In contrast, L-dopa reduced connectivity between all three caudate seeds and regions of the “default mode” network, particularly PCC. Furthermore, L-dopa-related decreases in FC between caudate and PCC were inversely correlated with an L-dopa-related increase in FC with left vIPFC (Fig. 5). Highly similar patterns of FC and L-dopa related changes in FC were observed when we used a set of anatomically defined, probability-weighted ROIs (Figs. 6, 7). Further exploratory examination of the posterior cingulate FC revealed a striking reduction of connectivity within the default mode network as a result of L-dopa administration (Fig. 8). Not only did L-dopa reduce striatal involvement within the default mode network, but it also reduced connectivity within PCC and between PCC and medial PFC.

L-Dopa and motor and cognitive functional connectivity

Acute administration of a low dose (100 mg) of L-dopa increased connectivity between putamen and brainstem and cerebellum, relative to placebo. This observation is consistent with neuroimaging studies demonstrating that L-dopa and

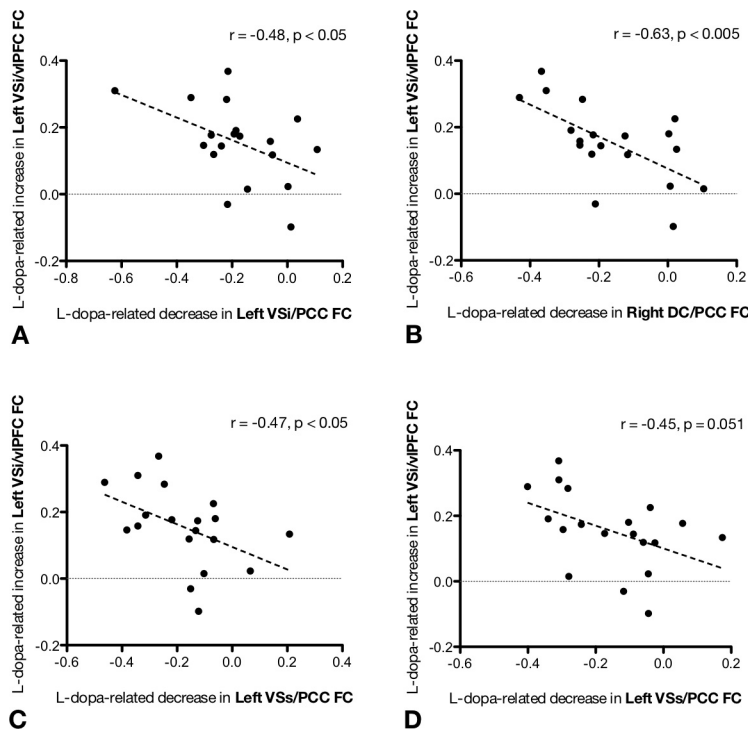


Figure 5. **A–D**, L-Dopa-related increase in VSi-vIPFC connectivity is inversely related to the L-dopa-related decrease in connectivity with PCC. We observed a significant inverse correlation between the L-dopa-related changes in connectivity: the greater the L-dopa-related increase in connectivity between VSs and PFC, the greater the L-dopa-related decrease in connectivity between the VSs and PCC for the same participant. Across participants, there were significant inverse correlations between the L-dopa-related changes in connectivity: the greater the L-dopa-related increase in FC between VSi and vIPFC, the greater the L-dopa-related decrease in FC for the same participant between left VSi and PCC (**A**), between right DC and PCC (**B**), between right VSs and PCC (**C**), and between left VSs and PCC (**D**).

other dopaminergic manipulations improve motor performance and normalize task-evoked activity in primary and secondary cortical motor areas, brainstem and cerebellum in both healthy and PD populations (Haslinger et al., 2001; Buhmann et al., 2003; Hershey et al., 2004; Asanuma et al., 2006; Palmer et al., 2009). Although earlier loop models of striatal motor networks (Alexander et al., 1986; Haber, 2003) did not consider subcortical interactions between striatum and cerebellum, recent studies have provided evidence of cerebellar input to the striatum, via a cerebello-thalamo-striatal pathway (Ichinohe et al., 2000; Hoshi et al., 2005). Moreover, interactions between striatal and cerebellar networks are increasingly implicated in movement disorders (Yu et al., 2007; Neychev et al., 2008) as well as in psychiatric conditions such as ADHD (Krain and Castellanos, 2006; Brennan and Arnsten, 2008).

L-Dopa also increased FC between the VSi, corresponding to the nucleus accumbens, and left vIPFC, relative to placebo. This observation mirrors the findings of a recent study (Nagano-Saito et al., 2008), in which DA depletion was associated with decreased connectivity between right dIPFC and dorsal caudate, and between both right and left vIPFC and the ventral striatum during a set-switching task. DA depletion also eliminated a positive relationship between frontostriatal FC and task performance, observed in the control (undepleted) condition. Conversely, studies have demonstrated improved performance on cognitive tasks subserved by frontostriatal circuits as a result of increased DA levels (Cools, 2006). Together, these studies suggest that FC and neuronal function within frontostriatal circuits is subject to modulation by dopaminergic signals from the striatum.

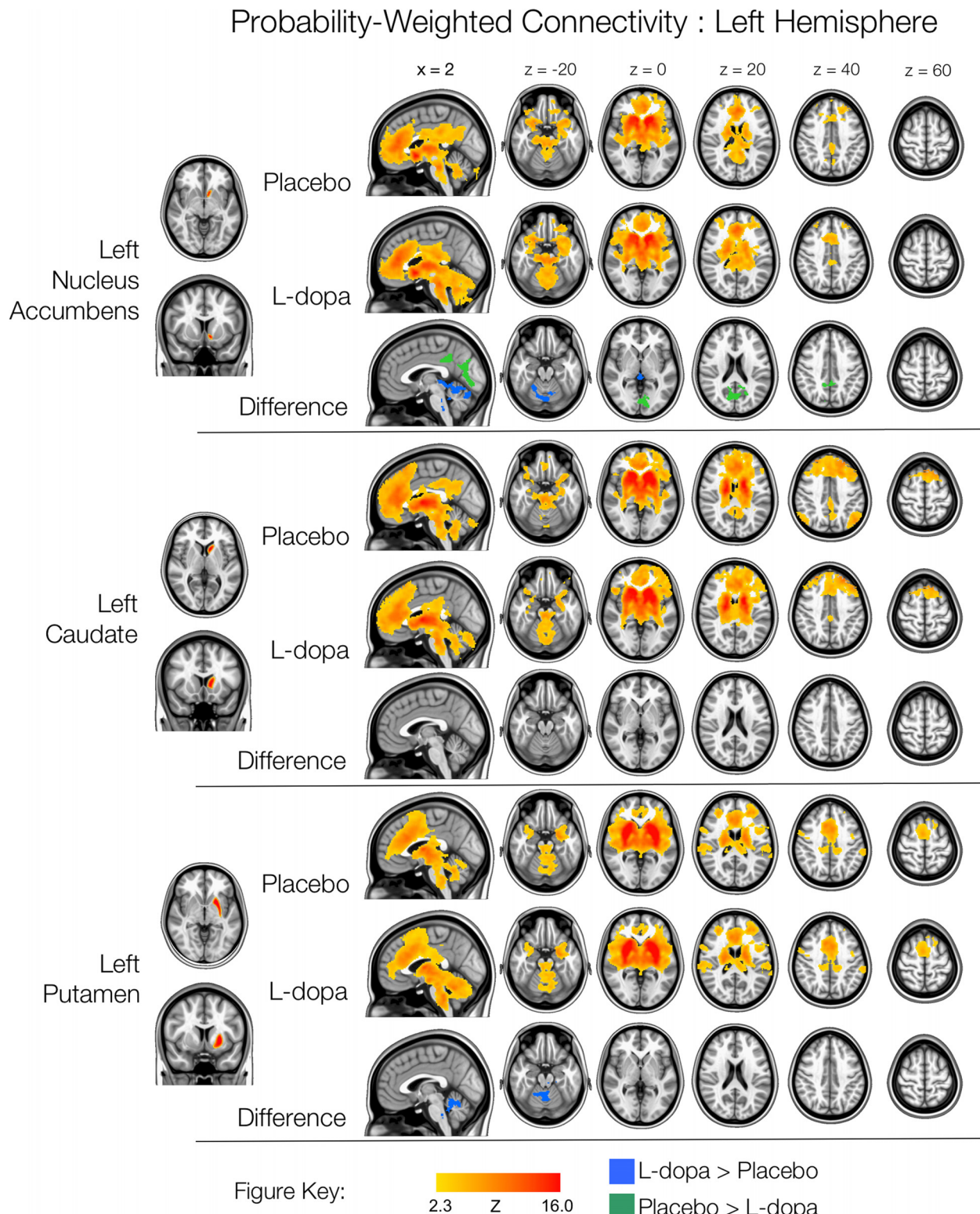


Figure 6. Left hemisphere probability-weighted functional connectivity. Thresholded Z-score maps of positive functional connectivity for each condition, and significant L-dopa-related increases and decreases in functional connectivity, for each of the three probability-weighted ROIs. Images are displayed according to radiological convention (left is right).

L-Dopa and the default mode network

Previous studies have demonstrated that activity (Shulman et al., 1997; McKiernan et al., 2003) and connectivity (Fransson, 2006) within the default mode network are reduced during task performance. The reduction in activity or connectivity typically occurs in association with increased activation in

task-relevant regions, such as dorsal ACC and lateral PFC (Fransson, 2006; Tomasi et al., 2006). Failure to suppress default mode activity during task performance, coupled with decreased task-evoked activation in prefrontal areas has been related to impaired behavioral performance (slower RTs, increased errors) (Polli et al., 2005; Weissman et al., 2006). Do-

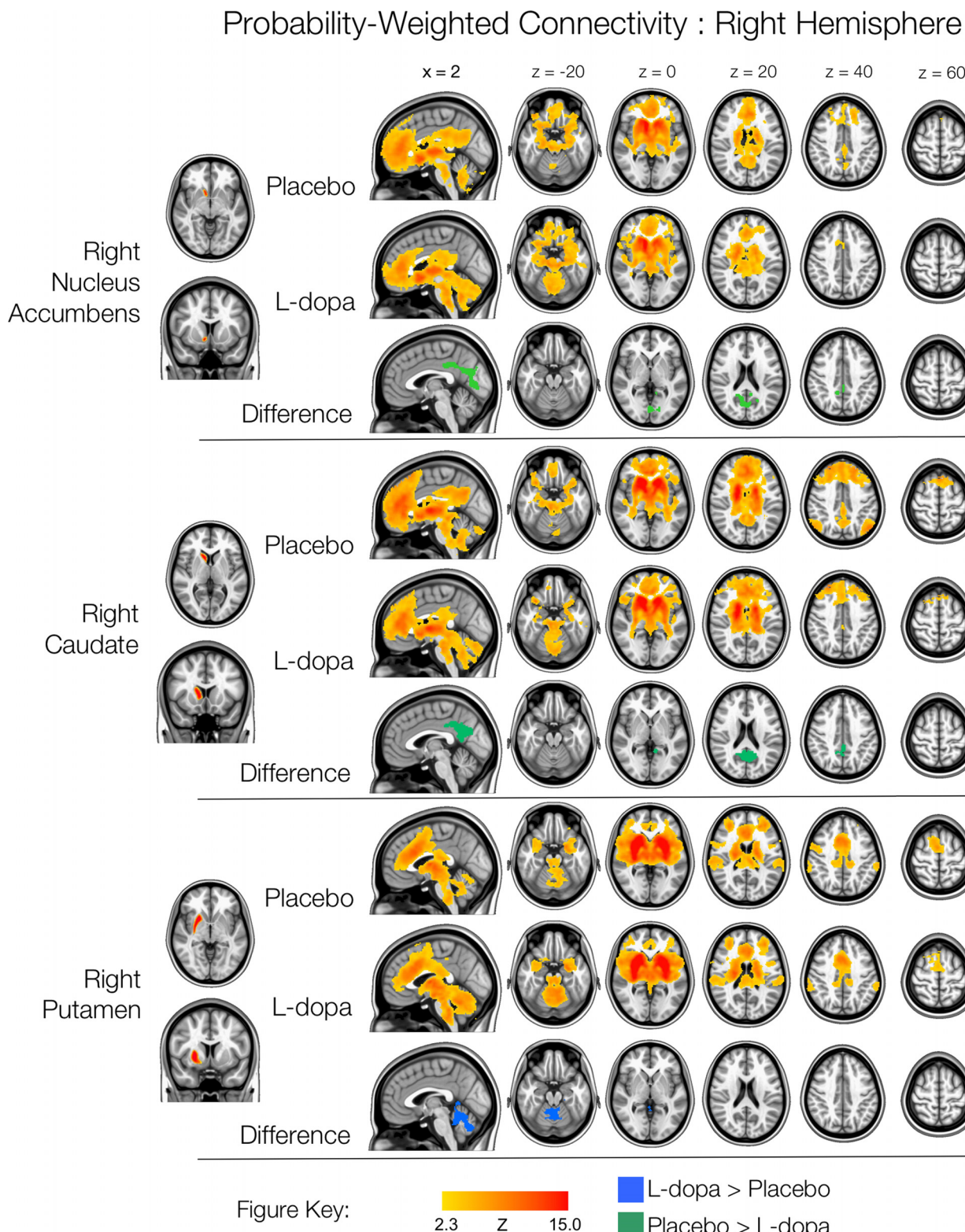


Figure 7. Right hemisphere probability-weighted functional connectivity. Thresholded Z-score maps of positive functional connectivity for each condition, and significant L-dopa-related increases and decreases in functional connectivity, for each of the three probability-weighted ROIs. Images are displayed according to radiological convention (left is right).

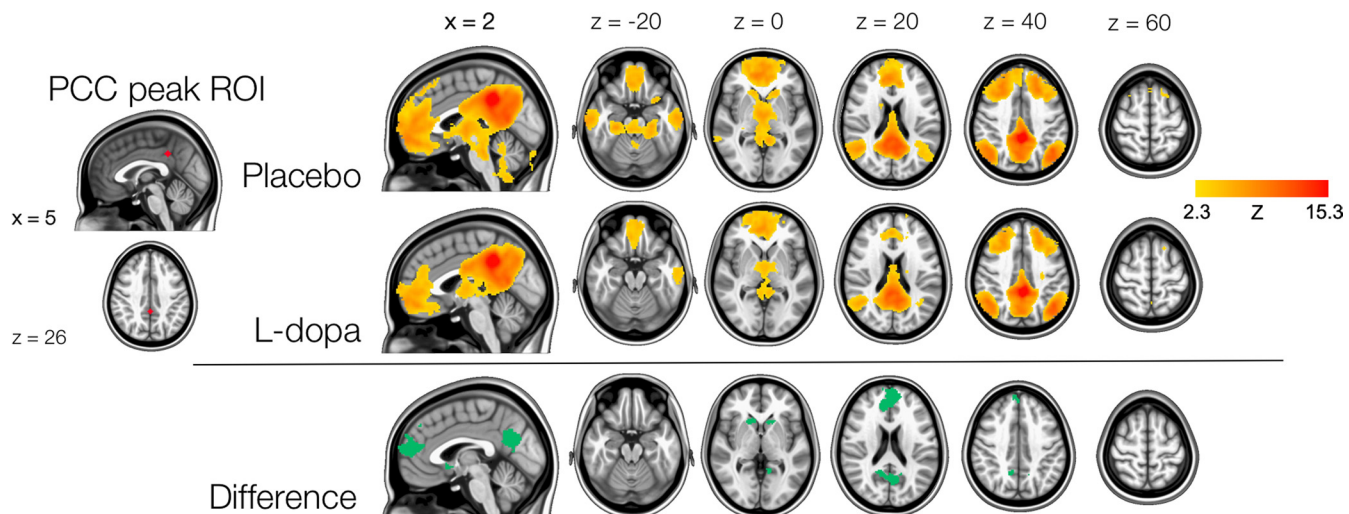
paminergic manipulations may have similar effects. Nagano-Saito et al. (2008) demonstrated that under conditions of DA depletion, task-related suppression of default mode network activity was reduced, as was FC between PFC and striatum. They also observed a trend toward slower task performance in

the DA depleted condition, relative to the undepleted condition. In our study, we augmented, rather than depleted DA, and, as would be predicted, our findings mirrored those of Nagano-Saito et al. Not only did L-dopa reduce FC within the default mode network, the reduction of FC between PCC and

Table 3. Significant changes in functional connectivity for L-dopa, relative to placebo, for each of the probability-weighted ROIs (min Z > 2.3; cluster significance: $p < 0.05$, corrected), as shown in Figures 6 and 7

| | | mm ³ | BA | Peak voxel | | |
|--|---|-----------------|------------------------|------------|-----|-----|
| | | | | x | y | z |
| L-Dopa-related increases in functional connectivity | | | | | | |
| L putamen | L cerebellum (lobules III, IV, V), cerebellar vermis (lobules VI), brainstem (pons) | 1378 | | -12 | -40 | -34 |
| R putamen | L cerebellum (lobules III, IV, V, VIIIB, IX), vermis (lobules VI, VIII, VIIIIA), brainstem (pons) | 2173 | | 0 | -70 | -36 |
| L nucleus accumbens | BL cerebellum (lobules IV, V, VI, IX, X), vermis (lobules VI), brainstem (pons) | 845 | | -12 | -66 | -16 |
| | | 1122 | | -12 | -36 | -36 |
| L-Dopa-related decreases in functional connectivity | | | | | | |
| R caudate | BL PCC | 2005 | 29, 30, 31 | -8 | -50 | 12 |
| L nucleus accumbens | BL PCC, medial occipital cortex | 2121 | 23, 30, 31, 17, 18, 19 | 10 | -76 | 36 |
| R nucleus accumbens | BL PCC, medial occipital cortex | 2379 | 23, 30, 31, 17, 18, 19 | 4 | -32 | 34 |

BA, Brodmann area; BL, bilateral; L, left; R, right.

**Figure 8.** L-Dopa reduces functional connectivity within the default mode network. The iterative connectivity analysis, which examined the FC of the PCC region that demonstrated reduced connectivity with the right hemisphere probability-weighted caudate ROI (seed location shown on left off figure). The figure displays the thresholded Z-score maps of positive functional connectivity for each condition, and significant L-dopa-related increases and decreases in functional connectivity for this PCC seed ROI. A significant reduction in the connectivity of the default mode network in the L-dopa condition, relative to placebo, was observed. Images are displayed according to radiological convention (left is right).

three of the caudate seeds (right dorsal caudate, right superior ventral striatum and left inferior ventral striatum) was significantly inversely related to the extent to which L-dopa increased FC between left nucleus accumbens (VSi) and right vLPFC.

How might DA bring about this bidirectional effect? Bamford and colleagues (2004a,b) propose that DA alters the signal-to-noise ratio within corticostriatal loops by reinforcing active corticostriatal synaptic connections and inhibiting inactive ones. Similar hypotheses have been proposed regarding the role of DA throughout the brain (Rolls et al., 1984; Kischka et al., 1996; Cepeda and Levine, 1998; Nicola et al., 2004), and regarding the role of DA in combination with norepinephrine (Arnsten, 2007). Speculatively, reduced connectivity within the default mode network, coupled with increased striatal-PFC or striatal-cerebellar connectivity might reflect such increased signal-to-noise. Striatal DA circuits may provide a mechanism for the active suppression of the default mode network under conditions that require increased processing of external stimuli (signal) relative to internal, self-directed processing (noise).

Limitations

Although we observed L-dopa-related increases in FC between dorsal putamen, a region hypothesized to serve primarily motor

functions, and regions of the brainstem and cerebellum, we did not observe increased FC between putamen and primary or secondary motor cortical regions. One possible explanation is that we did not observe the same primary motor connectivity for the dorsal putamen seeds as did Di Martino et al. (2008; see supplemental Results A, available at www.jneurosci.org as supplemental material, for further details). A second possibility is that, as a subtherapeutic dose of L-dopa was administered, the effects of L-dopa on striatal motor networks were subtle. Larger effects extending to primary and secondary motor cortices may be observed at different doses, which should be assessed in a future study.

We demonstrated robust effects of L-dopa on striatal FC that we have hypothesized were related to the modulatory effects of DA on striatal motor and cognitive function. We and others have observed significant alterations in performance on behavioral tasks with the same dosage of L-dopa (Kischka et al., 1996; Angwin et al., 2004; Copland et al., 2009). However, there are interindividual differences in the effects of DA challenge on a given cognitive or motor function that reflect interindividual differences in baseline DA levels. Furthermore, inverse-U-shaped relationships exist both between DA levels

and BOLD/PET activation levels, and between DA levels and behavioral performance (e.g., Cools, 2006; Rowe et al., 2008; Cools et al., 2009). Because we had no external measures of the impact of L-dopa on motor or cognitive performance, we cannot know whether the observed changes in FC were associated with improvement or decrements in performance. In fact, L-dopa-related reductions of FC between PCC and other default mode network components (e.g., medial PFC) may even have a negative impact on task performance, as suggested by a recent study relating working memory performance to default mode connectivity (Hampson et al., 2006). Future studies should address the potential effects of smaller and larger doses of L-dopa on both FC and performance on motor and cognitive tasks subserved by striatal circuits, as well as how individual differences impact the dose–response relationship.

Controversy surrounding the nature of negative relationships between networks (anticorrelations) in FC analyses persists (Skudlarski et al., 2008; Murphy et al., 2009). However, recent work examining the test-retest reliability of anticorrelations (Shehzad et al., 2009) and the emergence of anticorrelations in a computational model of cortical connectivity (Ghosh et al., 2008) encourages confidence in their fidelity. Although we did not explicitly discuss the patterns of negative functional connectivity associated with each our ROIs, they were consistent with those previously observed by Di Martino et al. (2008), and are shown in supplemental Figures S1–S4, available at www.jneurosci.org as supplemental material. Interestingly, we observed no significant effects of L-dopa on negative connectivity, suggesting that relationships within the functionally connected networks we observed were more sensitive to L-dopa than relationships between those networks and their negatively correlated counterparts. Further studies examining the impact of pharmacological manipulations on the negative relationships among networks are required to test this hypothesis. Such studies may shed light on the neurophysiological bases of negative relationships among networks.

Implications and future directions

Our observation of an L-dopa-related reduction of FC within the default mode network may help advance our understanding of previous studies that have demonstrated significant differences in default mode FC in conditions such as ADHD (Castellanos et al., 2008), and in normal aging (Andrews-Hanna et al., 2007; Damoiseaux et al., 2008). Dysregulation of catecholaminergic neurotransmission is thought to play a role in these conditions (Laruelle et al., 2003; Bäckman et al., 2006; Brennan and Arnsten, 2008; Tripp and Wickens, 2008; but see Gonon, 2009). Here, we have provided initial support for the hypothesis that DA contributes to the regulation of FC in the brain, bolstering the suggestion that the abnormalities in default mode connectivity in these conditions may be related to DA dysregulation. One way in which future studies might further examine this hypothesis is to examine whether a DA challenge normalizes FC of the default mode network in a population such as older adults.

Summary

We observed robust effects of acute low-dose L-dopa administration on striatal networks implicated in motor and cognitive function, in a sample of healthy young adults. Our results suggest that, although large-scale patterns of resting state FC are spatially and temporally stable, alterations of network coherence may result from changes in neurochemical state. Connectivity within the

default mode network was particularly sensitive to DA manipulation. These findings are consistent with a role for DA in the modulation of FC observed during task performance, as well as in the altered FC observed in pathological conditions.

References

- Achard S, Bullmore ET (2007) Efficiency and cost of economical brain functional networks. *PLoS Comput Biol* 3:e17.
- Alexander GE, DeLong MR, Strick PL (1986) Parallel organization of functionally segregated circuits linking basal ganglia and cortex. *Annu Rev Neurosci* 9:357–381.
- Andersson JLR, Jenkinson M, Smith SM (2007a) Non-linear optimisation. FMRIB technical report TR07JA1.
- Andersson JLR, Jenkinson M, Smith SM (2007b) Non-linear registration, aka spatial normalisation. FMRIB technical report TR07JA2.
- Andrews-Hanna JR, Snyder AZ, Vincent JL, Lustig C, Head D, Raichle ME, Buckner RL (2007) Disruption of large-scale brain systems in advanced aging. *Neuron* 56:924–935.
- Angwin AJ, Chenery HJ, Copland DA, Arnott WL, Murdoch BE, Silburn PA (2004) Dopamine and semantic activation: an investigation of masked direct and indirect priming. *J Int Neuropsychol Soc* 10:15–25.
- Arnsten AF (2007) Catecholamine and second messenger influences on prefrontal cortical networks of “representational knowledge”: a rational bridge between genetics and the symptoms of mental illness. *Cereb Cortex* 17 [Suppl 1]:i6–i15.
- Asanuma K, Tang C, Ma Y, Dhawan V, Mattis P, Edwards C, Kaplitt MG, Feigin A, Eidelberg D (2006) Network modulation in the treatment of Parkinson’s disease. *Brain* 129:2667–2678.
- Bäckman L, Nyberg L, Lindenberger U, Li SC, Farde L (2006) The correlative triad among aging, dopamine, and cognition: current status and future prospects. *Neurosci Biobehav Rev* 30:791–807.
- Bamford NS, Zhang H, Schmitz Y, Wu NP, Cepeda C, Levine MS, Schmauss C, Zakharenko SS, Zablow L, Sulzer D (2004a) Heterosynaptic dopamine neurotransmission selects sets of corticostriatal terminals. *Neuron* 42:653–663.
- Bamford NS, Robinson S, Palmiter RD, Joyce JA, Moore C, Meshul CK (2004b) Dopamine modulates release from corticostriatal terminals. *J Neurosci* 24:9541–9552.
- Biswal B, Yetkin FZ, Haughton VM, Hyde JS (1995) Functional connectivity in the motor cortex of resting human brain using echo-planar MRI. *Magn Reson Med* 34:537–541.
- Bond A, Lader M (1974) The use of analog scales in rating subjects feelings. *Br J Med Psychol* 47:211–218.
- Brennan AR, Arnsten AF (2008) Neuronal mechanisms underlying attention deficit hyperactivity disorder: the influence of arousal on prefrontal cortical function. *Ann N Y Acad Sci* 1129:236–245.
- Buhmann C, Glauche V, Stürenburg HJ, Oechsner M, Weiller C, Büchel C (2003) Pharmacologically modulated fMRI–cortical responsiveness to levodopa in drug-naïve hemiparkinsonian patients. *Brain* 126:451–461.
- Castellanos FX, Margulies DS, Kelly C, Uddin LQ, Ghaffari M, Kirsch A, Shaw D, Shehzad Z, Di Martino A, Biswal BB, Sonuga-Barke EJS, Rotrosen J, Adler LA, Milham MP (2008) Cingulate-precuneus interactions: a new locus of dysfunction in adult attention-deficit/hyperactivity disorder. *Biol Psychiatry* 63:332–337.
- Cepeda C, Levine MS (1998) Dopamine and N-methyl-D-aspartate receptor interactions in the neostriatum. *Dev Neurosci* 20:1–18.
- Cools R (2006) Dopaminergic modulation of cognitive function—implications for L-DOPA treatment in Parkinson’s disease. *Neurosci Biobehav Rev* 30:1–23.
- Cools R, Frank MJ, Gibbs SE, Miyakawa A, Jagust W, D’Esposito M (2009) Striatal dopamine predicts outcome-specific reversal learning and its sensitivity to dopaminergic drug administration. *J Neurosci* 29:1538–1543.
- Copland DA, McMahon KL, Silburn PA, de Zubicaray GI (2009) Dopaminergic neuromodulation of semantic processing: a 4-T fMRI study with levodopa. *Cereb Cortex*, in press.
- Cox RW (1996) AFNI: software for analysis and visualization of functional magnetic resonance neuroimages. *Comput Biomed Res* 29:162–173.
- Damoiseaux JS, Beckmann CF, Arigita EJ, Barkhof F, Scheltens P, Stam CJ, Smith SM, Rombouts SA (2008) Reduced resting-state brain activity in the “default network” in normal aging. *Cereb Cortex* 18:1856–1864.
- Di Martino A, Scheres A, Margulies DS, Kelly AM, Uddin LQ, Shehzad Z, Biswal B, Walters JR, Castellanos FX, Milham MP (2008) Functional

- connectivity of human striatum: a resting state fMRI study. *Cereb Cortex* 18:2735–2747.
- Drevets WC, Price JC, Kupfer DJ, Kinahan PE, Lopresti B, Holt D, Mathis C (1999) PET measures of amphetamine-induced dopamine release in ventral versus dorsal striatum. *Neuropsychopharmacology* 21:694–709.
- Fox MD, Snyder AZ, Vincent JL, Corbetta M, Van Essen DC, Raichle ME (2005) The human brain is intrinsically organized into dynamic, anticorrelated functional networks. *Proc Natl Acad Sci U S A* 102:9673–9678.
- Fransson P (2005) Spontaneous low-frequency BOLD signal fluctuations: an fMRI investigation of the resting-state default mode of brain function hypothesis. *Hum Brain Mapp* 26:15–29.
- Fransson P (2006) How default is the default mode of brain function? Further evidence from intrinsic BOLD signal fluctuations. *Neuropsychologia* 44:2836–2845.
- Ghosh A, Rho Y, McIntosh AR, Kötter R, Jirsa VK (2008) Noise during rest enables the exploration of the brain's dynamic repertoire. *PLoS Comput Biol* 4:e1000196.
- Gonon F (2009) The dopaminergic hypothesis of attention-deficit/hyperactivity disorder needs re-examining. *Trends Neurosci* 32:2–8.
- Graybiel AM (2008) Habits, rituals, and the evaluative brain. *Annu Rev Neurosci* 31:359–387.
- Greicius MD, Srivastava G, Reiss AL, Menon V (2004) Default-mode network activity distinguishes Alzheimer's disease from healthy aging: evidence from functional MRI. *Proc Natl Acad Sci U S A* 101:4637–4642.
- Haber SN (2003) The primate basal ganglia: parallel and integrative networks. *J Chem Neuroanat* 26:317–330.
- Hampson M, Driesen NR, Skudlarski P, Gore JC, Constable RT (2006) Brain connectivity related to working memory performance. *J Neurosci* 26:13338–13343.
- Haslinger B, Erhard P, Kämpfe N, Boecker H, Rummeny E, Schwaiger M, Conrad B, Ceballos-Baumann AO (2001) Event-related functional magnetic resonance imaging in Parkinson's disease before and after levodopa. *Brain* 124:558–570.
- Heimer L, Alheid GF (1991) Piecing together the puzzle of basal forebrain anatomy. *Adv Exp Med Biol* 295:1–42.
- Hershey T, Black KJ, Hartlein J, Braver TS, Barch DM, Carl JL, Perlmuter JS (2004) Dopaminergic modulation of response inhibition: an fMRI study. *Brain Res Cogn Brain Res* 20:438–448.
- Honey GD, Suckling J, Zelaya F, Long C, Routledge C, Jackson S, Ng V, Fletcher PC, Williams SC, Brown J, Bullmore ET (2003) Dopaminergic drug effects on physiological connectivity in a human cortico-striato-thalamic system. *Brain* 126:1767–1781.
- Hoshi E, Tremblay L, Féger J, Carras PL, Strick PL (2005) The cerebellum communicates with the basal ganglia. *Nat Neurosci* 8:1491–1493.
- Ichinohe N, Mori F, Shoumura K (2000) A di-synaptic projection from the lateral cerebellar nucleus to the laterodorsal part of the striatum via the central lateral nucleus of the thalamus in the rat. *Brain Res* 880:191–197.
- Jenkinson M, Smith S (2001) A global optimisation method for robust affine registration of brain images. *Med Image Anal* 5:143–156.
- Jenkinson M, Bannister P, Brady M, Smith S (2002) Improved optimization for the robust and accurate linear registration and motion correction of brain images. *Neuroimage* 17:825–841.
- Kahn I, Andrews-Hanna JR, Vincent JL, Snyder AZ, Buckner RL (2008) Distinct cortical anatomy linked to subregions of the medial temporal lobe revealed by intrinsic functional connectivity. *J Neurophysiol* 100:129–139.
- Kelly AM, Uddin LQ, Biswal BB, Castellanos FX, Milham MP (2008) Competition between functional brain networks mediates behavioral variability. *Neuroimage* 39:527–537.
- Kennedy DN, Lange N, Makris N, Bates J, Meyer J, Caviness VS Jr (1998) Gyri of the human neocortex: an MRI-based analysis of volume and variance. *Cereb Cortex* 8:372–384.
- Kischka U, Kammer T, Maier S, Weisbrod M, Thimm M, Spitzer M (1996) Dopaminergic modulation of semantic network activation. *Neuropsychologia* 34:1107–1113.
- Krain AL, Castellanos FX (2006) Brain development and ADHD. *Clin Psychol Rev* 26:433–444.
- Laruelle M, Kegeles LS, Abi-Dargham A (2003) Glutamate, dopamine, and schizophrenia: from pathophysiology to treatment. *Ann N Y Acad Sci* 1003:138–158.
- Li SJ, Biswal B, Li Z, Risinger R, Rainey C, Cho JK, Salmeron BJ, Stein EA (2000) Cocaine administration decreases functional connectivity in human primary visual and motor cortex as detected by functional MRI. *Magn Reson Med* 43:45–51.
- Makris N, Meyer JW, Bates JF, Yeterian EH, Kennedy DN, Caviness VS (1999) MRI-Based topographic parcellation of human cerebral white matter and nuclei II. Rationale and applications with systematics of cerebral connectivity. *Neuroimage* 9:18–45.
- Margulies DS, Kelly AM, Uddin LQ, Biswal BB, Castellanos FX, Milham MP (2007) Mapping the functional connectivity of anterior cingulate cortex. *Neuroimage* 37:579–588.
- Mattay VS, Tessitore A, Callicott JH, Bertolino A, Goldberg TE, Chase TN, Hyde TM, Weinberger DR (2002) Dopaminergic modulation of cortical function in patients with Parkinson's disease. *Ann Neurol* 51:156–164.
- McKiernan KA, Kaufman JN, Kucera-Thompson J, Binder JR (2003) A parametric manipulation of factors affecting task-induced deactivation in functional neuroimaging. *J Cogn Neurosci* 15:394–408.
- Montague PR, Hyman SE, Cohen JD (2004) Computational roles for dopamine in behavioural control. *Nature* 431:760–767.
- Murphy K, Birn RM, Handwerker DA, Jones TB, Bandettini PA (2009) The impact of global signal regression on resting state correlations: are anti-correlated networks introduced? *Neuroimage* 44:893–905.
- Nagano-Saito A, Leyton M, Monchi O, Goldberg YK, He Y, Dagher A (2008) Dopamine depletion impairs frontostriatal functional connectivity during a set-shifting task. *J Neurosci* 28:3697–3706.
- Neychev VK, Fan X, Mitev VI, Hess EJ, Jinnah HA (2008) The basal ganglia and cerebellum interact in the expression of dystonic movement. *Brain* 131:2499–2509.
- Nicola SM, Woodward Hopf F, Hjelmstad GO (2004) Contrast enhancement: a physiological effect of striatal dopamine? *Cell Tissue Res* 318:93–106.
- Olanow W, Schapira AH, Rascol O (2000) Continuous dopamine-receptor stimulation in early Parkinson's disease. *Trends Neurosci* 23:S117–126.
- Palmer SJ, Eigenraam L, Hoque T, McCaig RG, Troiano A, McKeown MJ (2009) Levodopa-sensitive, dynamic changes in effective connectivity during simultaneous movements in Parkinson's disease. *Neuroscience* 158:693–704.
- Polli FE, Barton JJ, Cain MS, Thakkar KN, Rauch SL, Manoach DS (2005) Rostral and dorsal anterior cingulate cortex make dissociable contributions during antisaccade error commission. *Proc Natl Acad Sci U S A* 102:15700–15705.
- Postuma RB, Dagher A (2006) Basal ganglia functional connectivity based on a meta-analysis of 126 positron emission tomography and functional magnetic resonance imaging publications. *Cereb Cortex* 16:1508–1521.
- Robbins TW (2005) Chemistry of the mind: neurochemical modulation of prefrontal cortical function. *J Comp Neurol* 493:140–146.
- Rolls ET, Thorpe SJ, Boytim M, Szabo I, Perrett DI (1984) Responses of striatal neurons in the behaving monkey. 3. Effects of iontophoretically applied dopamine on normal responsiveness. *Neuroscience* 12:1201–1212.
- Rowe JB, Hughes L, Ghosh BC, Eckstein D, Williams-Gray CH, Fallon S, Barker RA, Owen AM (2008) Parkinson's disease and dopaminergic therapy—differential effects on movement, reward and cognition. *Brain* 131:2094–2105.
- Schmahmann JD, Doyon J, Toga AW, Petrides M, Evans AC (2000) MRI atlas of the human cerebellum. San Diego: Academic.
- Shehzad Z, Kelly AM, Reiss PT, Gee DG, Gotimer K, Lee SH, Margulies DS, Roy AK, Biswal BB, Petkova E, Castellanos FX, Milham MP (2009) The resting brain: unconstrained yet reliable. *Cereb Cortex*, in press.
- Shulman GL, Fiez JA, Corbetta M, Buckner RL, Miezin FM, Raichle ME, Petersen SE (1997) Common blood flow changes across visual tasks. 2. Decreases in cerebral cortex. *J Cogn Neurosci* 9:648–663.
- Skudlarski P, Jaqannathan K, Calhoun VD, Hampson M, Skudlarska BA, Pearson G (2008) Measuring brain connectivity: diffusion tensor imaging validates resting state temporal correlations. *Neuroimage* 43:554–561.
- Sorg C, Riedl V, Mühlau M, Calhoun VD, Eichele T, Läer L, Drzezga A, Förstl H, Kurz A, Zimmer C, Wohlschläger AM (2007) Selective changes of resting-state networks in individuals at risk for Alzheimer's disease. *Proc Natl Acad Sci U S A* 104:18760–18765.
- Stark DE, Margulies DS, Shehzad ZE, Reiss P, Kelly AM, Uddin LQ, Gee DG, Roy AK, Banich MT, Castellanos FX, Milham MP (2008) Regional variation in interhemispheric coordination of intrinsic hemodynamic fluctuations. *J Neurosci* 28:13754–13764.

- Tomasi D, Ernst T, Caparelli EC, Chang L (2006) Common deactivation patterns during working memory and visual attention tasks: an intra-subject fMRI study at 4 Tesla. *Hum Brain Mapp* 27:694–705.
- Tripp G, Wickens JR (2008) Research review: dopamine transfer deficit: a neurobiological theory of altered reinforcement mechanisms in ADHD. *J Child Psychol Psychiatry* 49:691–704.
- Vaughan JT, Adriany G, Garwood M, Yacoub E, Duong T, DelaBarre L, Andersen P, Ugurbil K (2002) Detunable transverse electromagnetic (TEM) volume coil for high-field NMR. *Magn Reson Med* 47:990–1000.
- Vincent JL, Snyder AZ, Fox MD, Shannon BJ, Andrews JR, Raichle ME, Buckner RL (2006) Coherent spontaneous activity identifies a hippocampal-parietal memory network. *J Neurophysiol* 96:3517–3531.
- Weissman DH, Roberts KC, Visscher KM, Woldorff MG (2006) The neural bases of momentary lapses in attention. *Nat Neurosci* 9:971–978.
- Yu H, Sternad D, Corcos DM, Vaillancourt DE (2007) Role of hyperactive cerebellum and motor cortex in Parkinson's disease. *Neuroimage* 35:222–233.
- Zaitsev M, Hennig J, Speck O (2003) Automated onlinie EPI distortion correction for fMRI applications. In: Proceedings of the 11th annual meeting of the International Society for Magnetic Resonance in Medicine, July 10–16, 2003, Toronto, ON, Canada, 1042 [abstr].
- Zhou Y, Liang M, Tian L, Wang K, Hao Y, Liu H, Liu Z, Jiang T (2007) Functional disintegration in paranoid schizophrenia using resting-state fMRI. *Schizophr Res* 97:194–205.